An SH2-domain-containing kinase negatively regulates the phosphatidylinositol-3 kinase pathway

John Moniakis,[1] Satoru Funamoto,[1] Masashi Fukuzawa,[2] Jill Meisenhelder,[3] Tsuyoshi Araki,[2] Tomoaki Abe,[2] Ruedi Meili,[1] Tony Hunter,[3] Jeffrey Williams,[2] and Richard A. Firtel[1,4]

[1]Section of Cell and Developmental Biology and Center for Molecular Genetics, University of California, San Diego, La Jolla, California 92093-0634, USA; [2]Wellcome Trust Laboratories, School of Biological Sciences, University of Dundee, Dundee DD1 5EH, UK; [3]Molecular Biology and Virology Laboratory, The Salk Institute for Biological Studies, La Jolla, California 92037-1099, USA

SHK1 is a novel dual-specificity kinase that contains an SH2 domain in its C-terminal region. We demonstrate that SHK1 is required for proper chemotaxis and phagocytosis. Mutant *shk1* null cells lack polarity, move very slowly, and exhibit an elevated and temporally extended chemoattractant-mediated activation of the kinase Akt/PKB. GFP fusions of the PH domain of Akt/PKB or the PH-domain-containing protein CRAC, which become transiently associated with the plasma membrane after a global stimulation with a chemoattractant, remain associated with the plasma membrane for an extended period of time in *shk1* null cells. These results suggest that SHK1 is a negative regulator of the PI3K (phosphatidylinositol-3 kinase) pathway. Furthermore, when a chemoattractant gradient is applied to a wild-type cell, these PH-domain-containing proteins and the F-actin-binding protein coronin localize to its leading edge, but in an *shk1* null cell they become randomly associated with the plasma membrane and cortex, irrespective of the direction of the chemoattractant gradient, suggesting that SHK1 is required for the proper spatiotemporal control of F-actin levels in chemotaxing cells. Consistent with such functions, SHK1 is localized at the plasma membrane/cortex, and we show that its SH2 domain is required for this localization and the proper function of SHK1.

[*Key Words*: *Dictyostelium*; PI3K; SH2 domain; kinase; Akt/PKB]

Received December 5, 2000; revised version accepted January 25, 2001.

Class I phosphatidylinositol-3 kinases (PI3Ks) regulate diverse cellular processes including cell growth, apoptosis, endocytosis, phagocytosis, T-cell development, chemotaxis, and endocytosis (Buczynski et al. 1997; Leevers et al. 1999; Rameh and Cantley 1999; Vanhaesebroeck and Waterfield 1999; Vanhaesebroeck et al. 1999; Hirsch et al. 2000; Li et al. 2000; Sasaki et al. 2000). Leukocytes from mice lacking PI3Kγ or *Dictyostelium* cells lacking the genetically redundant Class I_A PI3Ks, PI3K1 and PI3K2 (*pi3k1/2* null cells) are defective in chemoattractant-mediated activation of protein kinase B (PKB or Akt), which is required for the establishment of cell polarity and chemotaxis in *Dictyostelium* (Meili et al. 1999, 2000; Vanhaesebroeck et al. 1999; Hirsch et al. 2000; Li et al. 2000; Salinas et al. 2000; Sasaki et al. 2000). In leukocytes, PKB is required for regulating proliferative/survival signals via many hematopoietic receptors (for review, see Coffer et al. 1998). PKB is activated in response to chemoattractants (Tilton et al. 1997), but its possible function in chemotaxis is not known.

[4]Corresponding author.
E-MAIL rafirtel@ucsd.edu; FAX (858) 534-7073.
Article and publication are at www.genesdev.org/cgi/doi/10.1101/gad.871001.

PI3K functions through the formation of PI(3,4,5)P_3 and PI(3,4)P_2, which act as plasma membrane docking sites for a subfamily of PH-domain-containing proteins (Fruman et al. 1999). GFP fusions containing the PH domains from mammalian and *Dictyostelium* PKB, or related PH domains from other proteins, rapidly translocate to the plasma membrane in response to global stimulation by chemoattractants and to the leading edge of chemotaxing neutrophils and *Dictyostelium* cells (Parent et al. 1998; Meili et al. 1999; Servant et al. 2000). Point mutations in the PKB PH domain that abrogate binding to the PI3K products PI(3,4,5)P_3 and PI(3,4)P_2 also abrogate translocation to the plasma membrane and activation in response to chemoattractants, whereas constitutive localization of PKB to the plasma membrane, by addition of a myristoylation site, leads to the constitutive activation of the protein (Alessi et al. 1996, 1997; Kohn et al. 1996; Andjelkovic et al. 1997; Frech et al. 1997; Klippel et al. 1997; Stockoe et al. 1997; Meili et al. 1999, 2000). These observations and studies with the *Dictyostelium* PH-domain-containing protein CRAC have led to a model in which localized activation of PI3K at the leading edge represents a key step in the establishment of axial polarity,

with F-actin present predominantly in the front of the cells and myosin II in the posterior, leading to the formation of a pseudopod in the direction of the chemoattractant source (Parent and Devreotes 1999; Firtel and Chung 2000; Rickert et al. 2000; Servant et al. 2000).

In this manuscript, we identify a novel SH2-domain-containing kinase, SHK1, that is required for proper chemotaxis and phagocytosis in *Dictyostelium*. We demonstrate that *shk1* null cells exhibit altered actin-cytoskeletal responses and elevated and extended chemoattractant-mediated PKB activation. By analysis of the kinetics of chemoattractant-mediated membrane translocation of PH-domain-containing proteins, we suggest that SHK1 is a key negative regulator of PI3K signaling pathways.

Results

An SH2-domain-containing, dual-specificity kinase is required for proper chemotaxis

The SHK1 (SH2-domain-containing kinase) was identified in a search of the *Dictyostelium* genomic and cDNA databases for SH2 domains (Fig. 1A). SHK1 has an N-terminal protein kinase domain, a central linker domain, an SH2 domain, and a short C-terminal tail (GenBank accession no. AJ297966). The kinase domain with a known function in the database most closely related to that of SHK1 is CTR1 (Q05609; 1.1e-44), a component of the *Arabidopsis* ethylene-response MAP kinase pathway; the SHK1 SH2 domain is most closely related to that of the mammalian PI3K adaptor protein p55 (Q64143), although no PI3K adapter proteins have been identified in *Dictyostelium* (Fig. 1B). To examine whether SHK1 is a serine/threonine and/or tyrosine kinase, SHK1 was expressed in *Escherichia coli* and used to phosphorylate the nonspecific substrates MBP and histone H2B. Phosphoamino acid analysis showed a predominance of phosphoserine and phosphothreonine with some phosphotyrosine; the ratio of the three phosphoamino acids was 60–61:37:2–3 (Ser:Thr:Tyr) using either MBP or Histone 2B as a substrate.

Disruption of SHK1 by homologous recombination results in cells that are unable to aggregate properly; cells form very small mounds and fruiting bodies (data not shown). Expression of FLAG-tagged SHK1 from the constitutive Actin 15 promoter rescues the *shk1* null cell

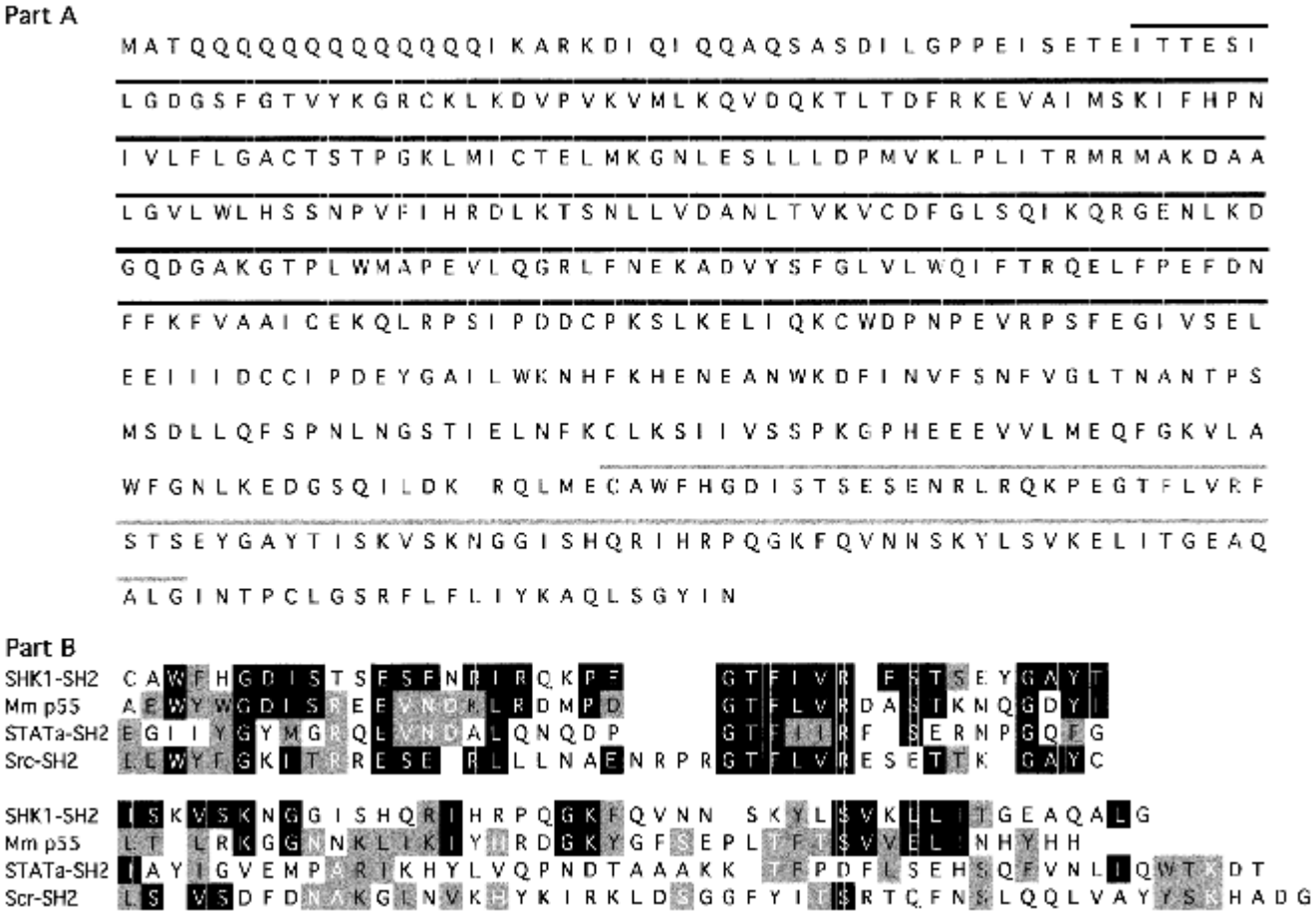

Figure 1. SHK1 primary amino acid sequence. (*A*) Sequence of SHK1. Putative kinase (black bar) and SH2 (gray bar) domains are indicated. (*B*) Sequence comparison of the SH2 domain of SHK1 with the SH2 domains of mouse p55, Q64143, human c-Src (P12931), and *Dictyostelium* STATa (Kawata et al. 1997).

phenotypes (data not shown). The observation that the cells do not aggregate properly suggests, among other possibilities, that *shk1* null cells are defective in chemotaxis. To examine this possibility directly, we studied the ability of *shk1* null cells to chemotax toward a micropipette containing the chemoattractant cAMP. When placed in a chemoattractant gradient, wild-type cells polarize and chemotax rapidly toward the chemoattractant source (Fig. 2A). In contrast, *shk1* null cells are unable to effectively polarize. Quantitation of chemotaxis using the DIAS computer program (Soll and Voss 1998; Wessels and Soll 1998) shows that *shk1* null cells chemotax very slowly and produce multiple pseudopodia, resulting in frequent changes in direction of cell movement (Fig. 2B). To test whether these defects are due to a general inability of *shk1* null cells to respond to the chemoattractant cAMP, we examined the ability of cAMP to induce expression of the aggregation-stage cAMP receptor cAR1. The *shk1* null cells show normal induction of cAR1, indicating that these cells can respond to cAMP (data not shown).

SHK1 is required for the proper regulation of the actin cytoskeleton

Examination of the actin cytoskeleton of aggregation-stage, chemotaxis-competent cells reveals that, in contrast to wild-type cells that have a highly polarized F-actin localization, *shk1* null cells have F-actin-enriched subdomains along the entire cortex of the cell (Fig. 2C). We examined whether the kinetics and level of chemoattractant-mediated F-actin polymerization were altered. Using a standard assay for quantitating F-actin levels (see Materials and Methods; Zigmond et al. 1997), we found that both wild-type and *shk1* null cells display indistinguishable kinetics and levels of F-actin accumulation after cAMP stimulation. Both strains show an ~2.2-fold increase upon cAMP stimulation, which peaks 5 sec after stimulation and then rapidly decreases to basal levels within 1 min (data not shown). Cells overexpressing SHK1 (SHK1^{OE} cells) show a small decrease in directionality and speed (Fig. 2B) but exhibit a normal F-actin distribution (data not shown). These results suggest that the spatial distribution of F-actin but not the overall magnitude of the actin response is perturbed in *shk1* null cells. In addition, *shk1* null cells exhibit a cytokinesis defect when the cells are grown in suspension. Under these conditions, *shk1* null cells become multinucleate over time (data not shown), suggesting that they are impaired in cytokinesis. When, however, *shk1* null cells are grown attached to a substratum in Petri dishes, they are predominantly mononucleate. This differential growth behavior between growth in suspension and on Petri dishes was first observed with myosin II null cells (Fukui et al. 1990). We expect that, like myosin II null cells, *shk1* null cells divide by traction-mediated cytofission on Petri dishes (Fukui et al. 1990). No cytokinesis defects were observed in SHK1^{OE} cells.

Because the spatial localization of F-actin in histologically fixed *shk1* null cells seems highly abnormal, we employed a living cell assay to examine the ability of cells to assemble actin in response to chemoattractant signaling. Coronin is an F-actin-binding protein that can be used as a green fluorescent protein (GFP) fusion protein to follow and visualize changes in the subcellular localization of F-actin in living cells (de Hostos et al. 1991; Gerisch et al. 1995). In response to global cAMP stimulation, coronin–GFP rapidly translocates to the cell cortex, with the level peaking at ~4–5 sec (Gerisch et al. 1995). In *shk1* null cells, the kinetics of increase are slower, with maximal cortical coronin levels at ~7–8 sec (Fig. 2D). Although this temporal difference is highly reproducible and indicates a difference between the two strains, a possibly more relevant assay with respect to the ability of cells to respond to chemoattractant gradients is whether F-actin can preferentially localize to the edge of the cell closest to the micropipette. When a cAMP chemoattractant gradient is established using a micropipette, coronin localizes to the edge closest to the micropipette tip in wild-type cells, concomitant with the formation of a new pseudopod (Fig. 2E,F; Gerisch et al. 1995). When the position of the micropipette is changed relative to the cell, there is a rapid redistribution of coronin to the location in the cell cortex proximal to the new chemoattractant source. This accompanies the loss of the old pseudopod and the formation of a new pseudopod (Fig. 2E). In contrast, although *shk1* null cells exhibit a change in the pattern of coronin localization, the localization is almost random; coronin–GFP is found in multiple subcellular domains, without a clear correspondence with the position of the micropipette and the direction of the chemoattractant gradient (Fig. 2E,F). We suggest that the inability of *shk1* null cells to produce a spatially localized F-actin response in reaction to a directional signal represents a significant defect in the ability of these cells to chemotax properly and is an important component of the *shk1* null phenotype. We note that the difference between the results of the quantitative biochemical measurement of F-actin polymerization in response to cAMP stimulation (no differences between wild-type and *shk1* null cells) and the coronin–GFP assay is probably caused by differences in what is measured by each assay. The biochemical assay measures total F-actin, irrespective of its subcellular localization (Zigmond et al. 1997), whereas the coronin–GFP assay visualizes, in real time, the subcellular localization of coronin, which correlates with F-actin localization in the cell's cytoskeleton (Gerisch et al. 1995). In addition, the biochemical assay is intrinsically less able to accurately measure kinetics because of the difficulty in taking accurate time points at intervals of less than 5 sec.

SHK1 is a negative regulator of PI3K-dependent pathways

The chemotaxis and cell polarity phenotypes of *shk1* null cells exhibit some similarities to those of *pkbA* null

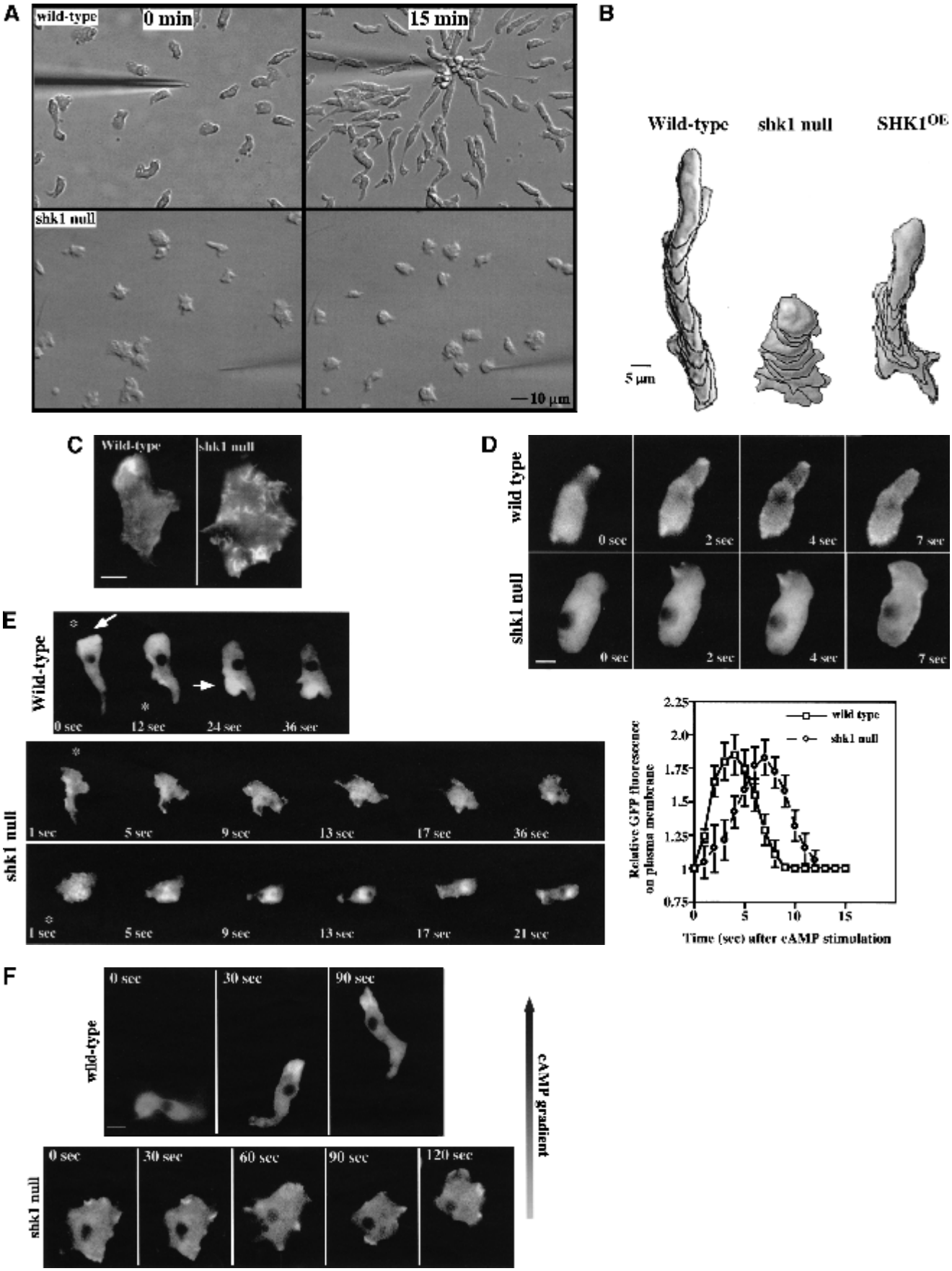
A
wild-type
0 min
15 min
shk1 null
10 μm
B
Wild-type
shk1 null
SHK1OE
5 μm
C
Wild-type
shk1 null
D
wild type
shk1 null
0 sec
2 sec
4 sec
7 sec
E
Wild-type
0 sec
12 sec
24 sec
36 sec
shk1 null
1 sec
5 sec
9 sec
13 sec
17 sec
36 sec
21 sec
Relative GFP fluorescence on plasma membrane
Time (sec) after cAMP stimulation
F
wild-type
0 sec
30 sec
90 sec
shk1 null
60 sec
120 sec
cAMP gradient

Table 1. *Chemotaxis parameters identified with the DIAS program*

Strain	Path length (μm)[a]	Speed (μm/min)[b]	Direction change (deg)[c]	Roundness (%)[d]	Directionality[e]
Wild type	59.2 ± 0.22	8.9 ± 0.25	26.5 ± 1.5	46.7 ± 2.4	0.71 ± 0.06
shk1 null	23.0 ± 1.3	4.1 ± 0.20	59.2 ± 1.1	69.1 ± 2.2	0.32 ± 0.01
SKH1 overexp.	50.2 ± 0.33	7.9 ± 0.26	31.1 ± 1.1	50.8 ± 5.4	0.59 ± 0.11

DIAS computer analysis was performed from digital time-lapse video DIC microscopy movies of the listed strains chemotaxing to cAMP. A 40× objective was used for the movies. The values indicate average values as calculated by the DIAS program.
[a]Indicates path length of the cell's centroid and not the actual linear distance traveled.
[b]Indicates speed of movement of the cell's centroid and not the actual distance traveled over a specificed time.
[c]Change in the direction (degrees) is a relative measure of the number and frequency of turns the cell makes. The parameter measures the change (degrees) in the position of the new pseudopod (leading edge) relative to the position of the cell's centroid. Higher numbers indicate more turns and less efficient chemotaxis.
[d]Roundness is an indication of the polarity of the cells. Larger numbers indicate the cells are more round and less polarized.
[e]Directionality is a measure of how straight the cells move. Cells moving in a straight line would have a directionality of 1.0.

cells. This finding, combined with the observation that the SH2 domain of SHK1 is most closely related to that of the PI3K adaptor p55, suggests a possible linkage between SHK1 and PI3K pathways. In *Dictyostelium* and mammalian cells, chemoattractant-mediated activation of PKB is PI3K-dependent (Alessi et al. 1996, 1997; Andjelkovic et al. 1997; Frech et al. 1997; Klippel et al. 1997; Stockoe et al. 1997; Meili et al. 1999, 2000). Wild-type cells show a rapid, receptor-mediated activation of PKB activity in response to chemoattractant stimulation that peaks at ~15 sec after stimulation and rapidly declines to basal levels by ~1 min (Fig. 3A; Meili et al. 1999). Interestingly, cAMP stimulation of *shk1* null cells results in a level of PKB activation that is ~fivefold higher than that observed for wild-type cells (Fig. 3A). In addition, instead of the activity decreasing rapidly, it remains elevated for a very extended period of time in *shk1* null cells. Conversely, overexpression of SHK1 leads to a reduction in the level of chemoattractant-stimulated PKB activation (Fig. 3A). As with activation of PKB in wild-type cells, this activation is PI3K-dependent, being inhibited by LY294002 (Fig. 3A; Meili et al. 1999). The high level of induction of PKB in *shk1* null cells and the suppression of activation in SHK1^{OE} cells suggest that SHK1 functions as a negative regulator of the PI3K pathway. Western blot analysis revealed that PKB protein levels are the same in wild-type and *shk1* null cells, indicating that the higher level of PKB activity is not caused by elevated levels of PKB protein (Fig. 3A). As the basal level of PKB activity is similar in all strains, it is probable that SHK1 regulates the pathway that is activated by chemoattractant stimulation and does not elevate the basal activity of the pathway.

Possible explanations for the hyperactivation of PKB in *shk1* null cells are that an elevated activation of PI3K and/or the lipid products of PI3K are more stable. One approach to measuring the biological consequences of a disruption of SHK1 on PI3K activity and the levels of the downstream products PI(3,4,5)P_3 and PI(3,4)P_2 is to examine the translocation of PH domains to the plasma membrane in response to chemoattractants. GFP fusions of the PH-domain-containing proteins CRAC (cytosolic regulator of adenylyl cyclase in *Dictyostelium*) and PhdA (S. Funamoto, K. Milan, R. Meili, and R.A. Firtel, unpubl.) or of the PH domains of PKB translocate to the plasma membrane in response to chemoattractant stimulation in a PI3K-dependent manner (Parent et al. 1998; Meili et al. 1999). In wild-type cells, CRAC–GFP and PKB-PH–GFP exhibit a rapid and transient translocation to the plasma membrane in response to a global stimulation with cAMP with localization peaking at ~5–6 sec and dissociation from the plasma membrane occurring by 10–12 sec (Fig. 3B; data for PKB–GFP not shown). In *shk1* null cells, we observe a similar, al-

Figure 2. Chemotaxis and cytoskeletal organization in *shk1* null cells. (*A*) Aggregation-competent cells (cells competent to respond chemotactically to cAMP, see Materials and Methods) were placed on glass slides, and a micropipette source of 150 μM cAMP was placed near the cells. Chemotaxis toward the micropipette was digitally recorded. (*B*) The pictures are images of cells at 1-min intervals. Chemotaxis parameters were quantified with the DIAS program. For DIAS program results see Table 1. (*C*) Aggregation-competent cells were fixed and stained with FITC-phalloidin as described previously (Chung and Firtel 1999). F-actin assembly was visualized by fluorescence microscopy. (*D*) Chemotaxis-competent wild-type and *shk1* null cells expressing full-length coronin–GFP fusion protein were placed on glass slides and stimulated globally with a pulse of 500 nM cAMP (final concentration). The ensuing membrane translocation in fluorescing cells was digitally recorded and quantified using the Metamorph program (Chung and Firtel 1999). (Note that the level of increase in fluorescence at the cortex is an indication of F-actin accumulation at the cell cortex and not a measure of the absolute change in F-actin in response to cAMP stimulation.) (*E*) Chemotaxis-competent wild-type and *shk1* null cells expressing full-length coronin–GFP fusion protein were provided with a micropipette source of 150 μM cAMP (*). The micropipette location was moved at the indicated times and changes to the coronin–GFP distribution in fluorescing cells were digitally recorded. (*F*) Chemotaxis-competent wild-type and *shk1* null cells expressing full-length coronin–GFP fusion protein were put on glass slides, and a cAMP gradient was established by placing a micropipette source of 150 μM cAMP near the cells. Chemotaxis of fluorescing cells was digitally recorded.

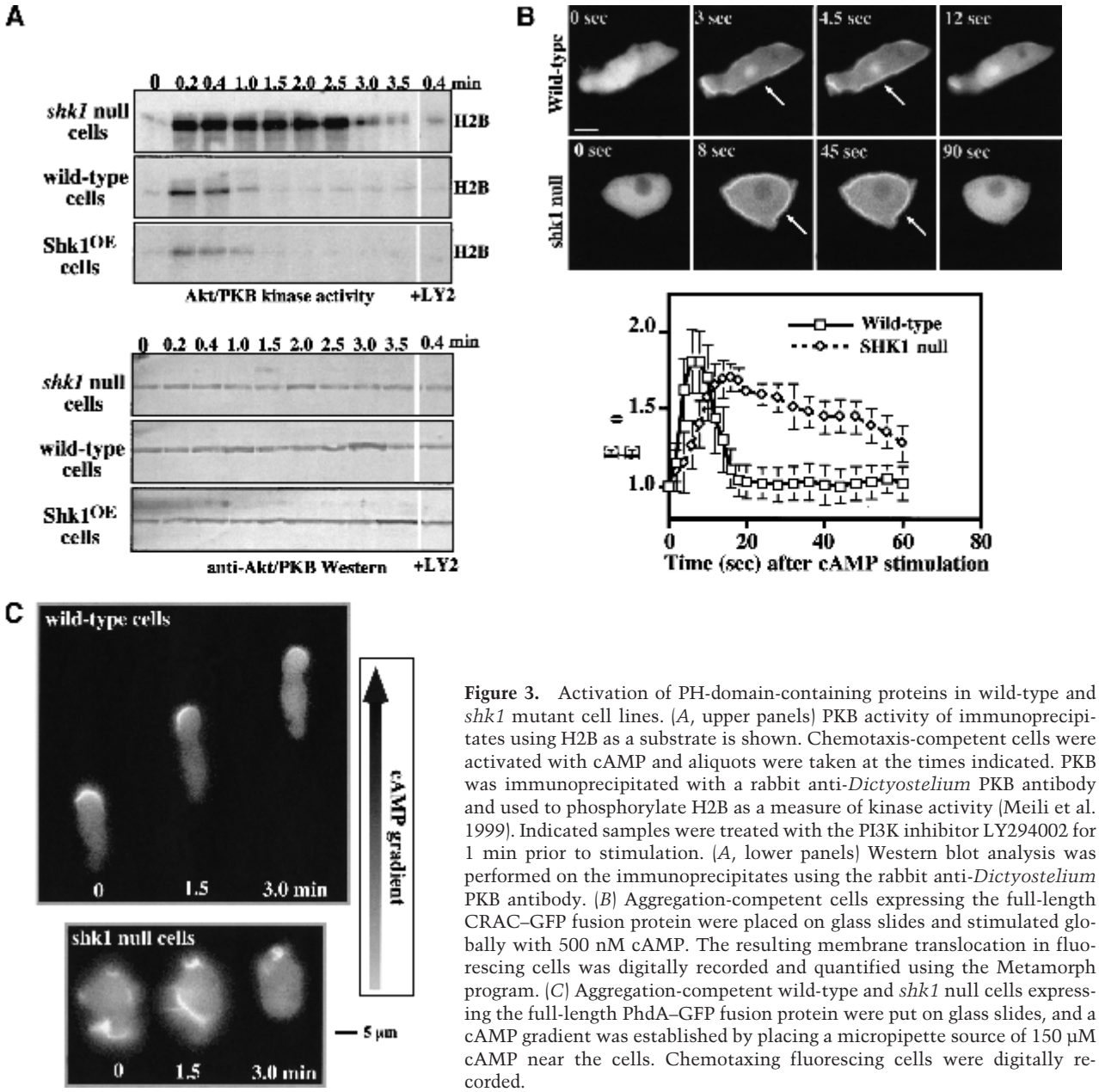

Figure 3. Activation of PH-domain-containing proteins in wild-type and *shk1* mutant cell lines. (*A*, upper panels) PKB activity of immunoprecipitates using H2B as a substrate is shown. Chemotaxis-competent cells were activated with cAMP and aliquots were taken at the times indicated. PKB was immunoprecipitated with a rabbit anti-*Dictyostelium* PKB antibody and used to phosphorylate H2B as a measure of kinase activity (Meili et al. 1999). Indicated samples were treated with the PI3K inhibitor LY294002 for 1 min prior to stimulation. (*A*, lower panels) Western blot analysis was performed on the immunoprecipitates using the rabbit anti-*Dictyostelium* PKB antibody. (*B*) Aggregation-competent cells expressing the full-length CRAC–GFP fusion protein were placed on glass slides and stimulated globally with 500 nM cAMP. The resulting membrane translocation in fluorescing cells was digitally recorded and quantified using the Metamorph program. (*C*) Aggregation-competent wild-type and *shk1* null cells expressing the full-length PhdA–GFP fusion protein were put on glass slides, and a cAMP gradient was established by placing a micropipette source of 150 μM cAMP near the cells. Chemotaxing fluorescing cells were digitally recorded.

though slightly slower, rate of translocation of CRAC–GFP and PKB-PH–GFP to the plasma membrane; however, the two GFP fusion proteins persist on the plasma membrane for a much longer period of time (note the difference in time scale in the two parts of Fig. 3B; data for PPKB-PH–GFP not shown). These data suggest that the phospholipid domains in the plasma membrane to which these two PH-domain-containing proteins bind may be present for only a very short time after chemoattractant stimulation in wild-type cells, but they persist for a much longer time in *shk1* null cells. Therefore, we propose that the elevated and prolonged activation of PKB likely results from a prolonged localization of PKB at the plasma membrane or from PKB localizing to the membrane, coming off the membrane, and then relocalizing. Extended membrane localization or relocalization to the plasma membrane would result in PKB being continually or repetitively activated by PDK1, respectively. Our findings are consistent with PH-domain lipid-binding sites being either significantly more stable in *shk1* null cells than in wild-type cells and/or with the level of PI3K activation being higher and remaining elevated for an extended period of time. However, we cannot rule out the possibility that a protein competing with the PH-domain-containing proteins that we tested for lipid binding may also be affected, producing the altered membrane localization kinetics that we observe.

In wild-type *Dictyostelium* cells, as in neutrophils, PH-domain-containing proteins such as CRAC, PhdA, and PKB localize to the leading edge in chemotaxing

cells (Parent et al. 1998; Meili et al. 1999; Servant et al. 2000; S. Funamoto, K. Milan, R. Meili, and R.A. Firtel, unpubl.). Figure 3C shows PhdA–GFP localizing to the leading edge in wild-type cells chemotaxing toward a micropipette containing cAMP. The three successive images taken at 1.5-min intervals depict the movement of the cell. In contrast, the membrane localization of PhdA–GFP is random with respect to the cAMP gradient in *shk1* null cells, and these cells exhibit little movement in the direction of the cAMP source. Our results suggest that *shk1* null cells have a defect in establishing a PI3K response that is localized and restricted to the leading edge when cells are placed in a chemoattractant gradient.

Phagocytosis is abnormal in shk1 *null cells*

We wondered whether the function of SHK1 extends beyond the proposed regulation of PI3K pathways in response to chemoattractants. We therefore examined phagocytosis, another actin-mediated cellular response, by quantifying the uptake of fluorescent beads or GFP-expressing *E. coli*, a natural food source for *Dictyostelium* amoebae. Figure 4 shows that the rate of bacteria uptake is considerably reduced in *shk1* null cells compared to wild-type cells. Consistent with these findings, *shk1* null cells grow more slowly on bacteria than do wild-type cells, as determined by the kinetics of clearing of bacteria from the medium (Fig. 4A). We did not observe localization of either CRAC–GFP or Akt-PH–GFP to phagocytic cups in either wild-type or *shk1* null cells upon binding and uptake of either bacteria or fluorescent beads (data not shown). It is possible that the translocation is too transient to be visualized. Alternatively, in *shk1* null cells, the phagocytosis defect may be an indirect effect of alterations in the actin cytoskeleton and its reorganization in *shk1* null cells and may not be directly regulated by PI3K (Buczynski et al. 1997).

The SH2 domain of SHK1 is required for SHK1 localization and function

To investigate where SHK1 might function within the cell, we studied the subcellular localization of SHK1 by staining for FLAG-tagged SHK1. Figure 5 demonstrates that SHK1 is predominantly cortical and is uniformly distributed around the periphery of cells in unstimulated cells. As the distribution is uniform, we suggest that SHK1 associates with the plasma membrane or a component of the cell cortex that is uniformly distributed and is not associated with the cytoskeleton. We investigated how SHK1 is associated with the cortex/plasma membrane and whether the localization domain is required for function. Figure 5 shows that a point mutation in the conserved arginine (Arg^{449}) of the SH2 domain ($SHK1^{R449A}$), which is required for phosphotyrosine binding (Fu and Zhang 1993; Shual et al. 1993), abrogates the ability of SHK1 to associate with the plasma membrane. This indicates that either SHK1 cortical association probably takes place through the binding of its SH2 domain to a tyrosine-phosphorylated protein or a functional SH2 domain confers another property on SHK1 that is required for its cortical localization. SH2 domains have been also shown to bind $PI(3,4,5)P_3$ (Rameh et al. 1995); however, addition of the PI3K inhibitor LY294002 at concentrations sufficient to block cAMP stimulation of Akt/PKB activation (Meili et al. 1999, 2000) did not affect the membrane localization of SHK1. We then tested whether the SH2 domain and/or its association with the plasma membrane are required for SHK1 function by expressing $SHK1^{R449A}$ in *shk1* null cells. Although FLAG-tagged $SHK1^{R449A}$ is expressed at the same

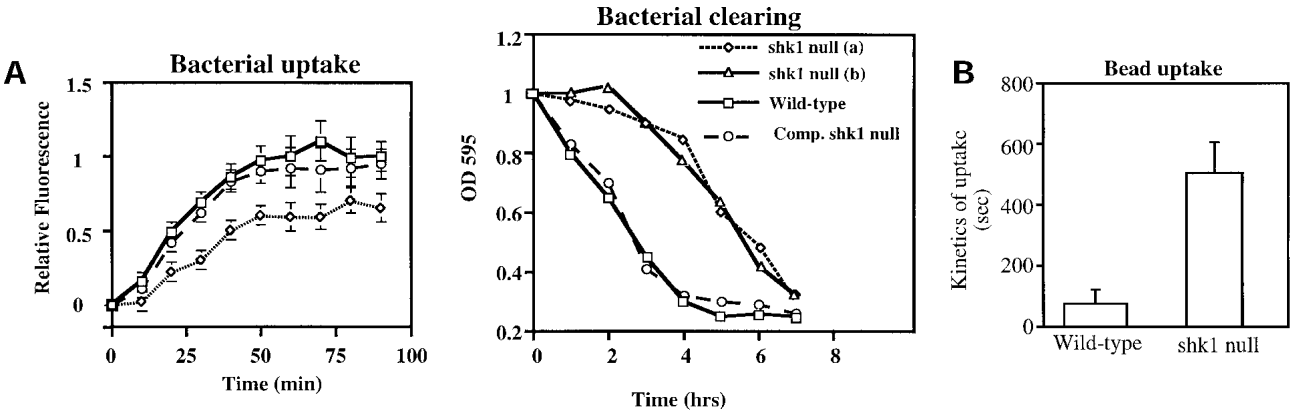

Figure 4. Phagocytosis in *shk1* mutant cell lines. (*A*) Cells grown axenically in log phase were adjusted to a concentration of 1×10^6 cells/mL in a suspension of GFP-tagged *E. coli*. Samples were taken at the time points shown, and *Dictyostelium* cells were isolated by differential centrifugation. The cells were fixed, and bacterial uptake was quantified fluorometrically. The label Comp. shk1 null refers to *shk1* null cells complemented with FLAG–SHK1. (*B*) The cells were adjusted to a concentration of 1×10^6 cells/mL in an *E. coli* suspension. The ability of the cells to grow on bacteria was quantified by measuring uptake and degradation of bacteria from the growth medium. (*C*) 1×10^5 axenically grown cells were placed on a glass slide in a suspension of Na/K phosphate buffer, and 2-μm FluoSphere beads were added to the suspension (to a final concentration of 2×10^3% solids). Bead internalization was monitored by DIC and fluorescence microscopy and digitally recorded.

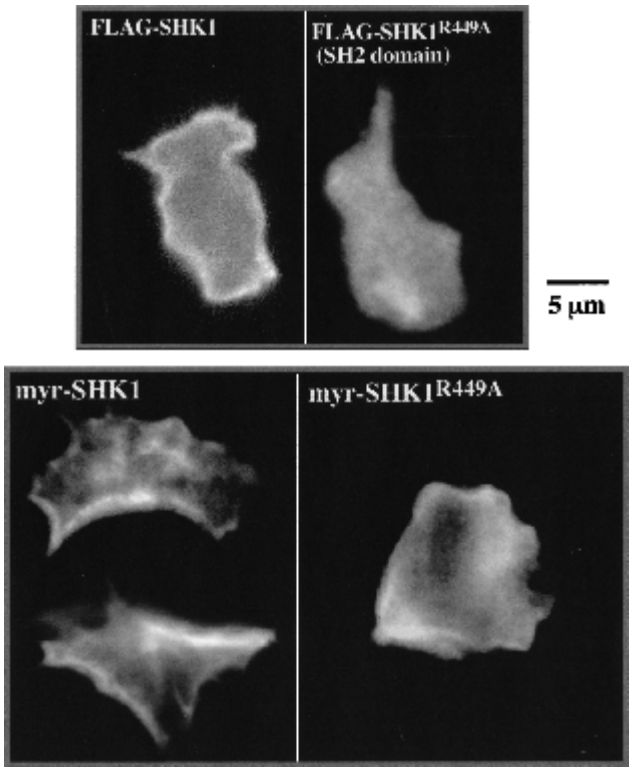

Figure 5. SHK1 localization. (*A*) *Dictyostelium* wild-type cells expressing FLAG–SHK1 and FLAG–SHK1^{R449A} (SH2 domain mutant R449A) fusion proteins were fixed and stained with anti-FLAG antibody. FLAG–SHK1 localization was visualized by indirect immunofluorescence. (*B*) *Dictyostelium shk1* null cells expressing myr-FLAG–SHK1 (FLAG–SHK1 with an N-terminal c-*Src* myristoylation site) and myr-FLAG–SHK1^{R449A} fusion proteins were fixed and stained with anti-FLAG antibody. Note that myr-FLAG–SHK1^{R449A} does not complement the *shk1* null phenotype and that *shk1* null cells are more spread and have a significant amount of random membrane ruffling and F-actin localization. This results in the abnormal-looking membrane localization of myr-FLAG–SHK1^{R449A}.

level as wild-type FLAG-tagged SHK1 protein expressed in *shk1* null cells, FLAG-tagged SHK1 (as described above) but not FLAG-tagged SHK1^{R449A} complements the null phenotype (data not shown). To examine if this is owing to an inability of SHK1^{R449A} to localize to the membrane, we added the c-*Src* myristoylation site (Buser et al. 1994; Sigal et al. 1994) to the N terminus of SHK1^{R449A} and wild-type SHK1 (myr-SHK1) carrying C-terminal FLAG tags and expressed them in *shk1* null cells. Although both proteins localize, at least partially, to the plasma membrane or cortex, as determined by indirect immunofluorescence staining (Fig. 5), only wild-type myr-SHK1 complements the null phenotype (data not shown). The results are consistent with the model that the SH2 domain is required for SHK1 function. We suspect from these studies that subcellular targeting of SHK1 to the plasma membrane or cortex is also required for SHK1 to be functional. However, as the SH2 domain is required to localize SHK1 to the plasma membrane/cortex as well as for SHK1 to function, we cannot directly determine if cortical/plasma membrane localization of SHK1 per se is essential.

Discussion

PI3K is an important regulator of cellular processes including chemotaxis. Our data suggest that SHK1 negatively regulates PI3K signaling pathways. *shk1* null cells are defective in the spatiotemporal regulation of F-actin assembly in response to chemoattractant stimulation, chemotaxis, and phagocytosis, another F-actin-mediated pathway. Our observations that PKB activation in response to cAMP stimulation, which is PI3K-dependent (Meili et al. 1999), is activated to a greater extent and is active for a more extended period of time in *shk1* null cells compared to wild-type cells are consistent with this model. In addition, the demonstration that the PH-domain-containing proteins CRAC and PKB exhibit a more prolonged membrane localization in response to cAMP signaling supports a model in which the PI3K products PI(3,4,5)P_3 and PI(3,4)P_2 are present at higher levels (consistent with an elevated PKB activation) and for an extended period of time in the plasma membrane. We found that a GFP fusion of the PH-domain-containing protein PhdA localizes almost randomly on the plasma membrane in *shk1* null cells that are in a chemoattractant gradient, rather than being localized at the leading edge. One possible explanation is that PI3K pathways are activated randomly along the cell's surface and SHK1 may be important in restricting the activation of the pathways to the leading edge. The *shk1* null phenotypes are very different from those of cells overexpressing PI3K1 (S. Funamoto and R.A. Firtel, unpubl.), suggesting that *shk1* null cells do not simply contain higher levels of PI3K protein.

The *shk1* null phenotypes are consistent with SHK1's cortical localization, suggesting this is where SHK1 functions in the cell. According to the presently understood mechanisms of regulation of PI3K activity, SHK1 could act either upstream of or directly on PI3K, modulating its activity under specific physiological conditions or in response to different stimuli. Alternatively, SHK1 might be a positive activator of the *Dictyostelium* phosphatidylinositol-3′ phosphatase PTEN (R. Meili and R.A. Firtel, unpubl.). These possibilities are depicted in the cartoon in Figure 6. It is also possible that SHK1 may regulate a yet to be identified component of the pathway. To date, we have not found an SHK1 homolog in the databases of other organisms. However, this is not unexpected, because *Dictyostelium* protein kinases capable of phosphorylating on tyrosine residues, even those that are monospecific tyrosine kinases, tend not to be closely related to metazoan kinases (Jungbluth et al. 1995; Adler et al. 1996; Nuckolls et al. 1996; Kim et al. 1999). We found that the SHK1 SH2 domain is most closely related to that of the p110α PI3K adaptor p55. This may be a chance occurrence, but it may also indicate an evolutionary relationship between the mechanisms by which PI3K pathways are regulated in *Dictyostelium* and mammalian cells. We note that the PI3K-dependent activa-

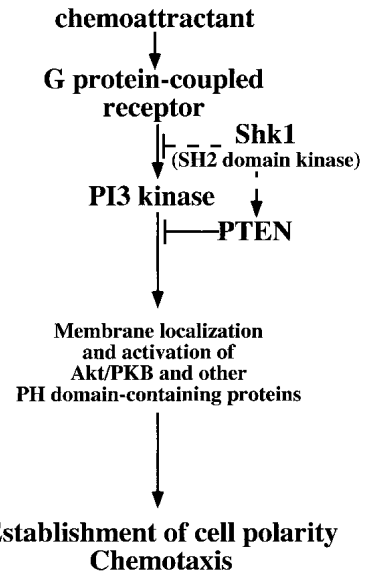

Figure 6. Function of SHK1. SHK1 may operate by inhibiting PI3K activity directly or by inhibiting PI3K upstream activators. SHK1 may also activate PTEN, a downstream inhibitor of the PI3K pathway. See text for details.

tion of PKB by chemoattractants in *Dictyostelium* is probably most closely related to activation of PKB by chemokines through the G-protein-linked PI3K, PI3Kγ, in leukocytes (Hirsch et al. 2000; Sasaki et al. 2000). Discovering whether SHK1 has more direct parallels to proteins in mammalian cells will require a more detailed characterization of the PI3Kγ pathways.

Paradoxically, both *shk1* null cells, which have elevated and extended chemoattractant-mediated PKB activity, and *pkbA* null cells exhibit impaired chemotaxis (Meili et al. 1999). We previously found that overexpression of PKB or the expression of a myristoyl-tagged PKB (which is found uniformly associated with the plasma membrane and constitutively active), leads to chemotaxis defects (Meili et al. 1999), although the phenotypes of *pkbA* null cells are not as severe as those exhibited by *shk1* null cells. We and others have previously suggested that proper spatial regulation and localization of PKB and PI3K activity at the leading edge may be crucial for the activation of cellular responses involved in chemotaxis (Meili et al. 1999; Parent and Devreotes 1999; Firtel and Chung 2000; Rickert et al. 2000). Chemotaxis of cells up a chemical gradient requires extension of the pseudopod and subsequent retraction of the posterior tail or uropod (Soll and Voss 1998; Parent and Devreotes 1999; Sanchez-Madrid and del Pozo 1999; Firtel and Chung 2000; Rickert et al. 2000). In addition, many of the known signaling pathways associated with chemotaxis, including the PKB pathway, involve a rapid activation followed by a rapid adaptation. It is thus possible that the very high level of activation of the PKB pathway, and its temporally extended activation, may disrupt the normal activation/adaptation pathway. We expect that all PI3K-mediated pathways that are stimulated by cAMP are affected in *shk1* null strains. Whereas we think that abnormal PKB activation contributes to the *shk1* null cell phenotypes, we expect *shk1* null cells to be defective in other pathways.

SHK1 may function as a general governor of PI3K activity or may be differentially regulated within the cell by physiological signals. Although we have not observed any change in SHK1 kinase activity, as assayed by immunoprecipitation and measurement of kinase activity of FLAG-tagged SHK1 expressed in *Dictyostelium* cells, in response to global chemoattractant stimulation (J. Moniakis and R.A. Firtel, unpubl.; see Materials and Methods), it is possible that SHK1 activity may be differentially regulated in various subdomains within the cell. For example, SHK1 function (possibly by controlling its kinase activity or its association with other proteins) may be inhibited at the leading edge in response to chemoattractant stimulation, resulting in a feedback loop activation of PI3K in this region, while inhibiting PI3K activity along the lateral sides and posterior of the cell, where we observe no localization of PH-domain-containing proteins when cells are placed in a chemoattractant gradient. Alternatively, SHK1 may provide a general form of inhibitory activity on the PI3K pathway (e.g., PTEN). Our results suggest that SHK1 requires a functional SH2 domain that does more than localize SHK1 to the plasma membrane. The SH2 domain may regulate the SHK1 kinase activity in some manner or, more likely, it may serve to localize SHK1 to other components in the pathway, including its substrate. SHK1 function may thus be regulated through its kinase activity and/or associated with the plasma membrane by controlling an upstream tyrosine kinase that phosphorylates the phosphotyrosine to which the SHK1 SH2 domain binds. Because unstimulated *shk1* null cells exhibit an abnormal actin cytoskeleton, we expect that SHK1 may also control basal PI3K function. The high level of general conservation of the role of PI3K in chemotaxis and phagocytosis in *Dictyostelium* and leukocytes suggests that SHK1 may have a counterpart in leukocytes that controls PI3K function similarly.

Materials and methods

Materials

Sodium orthovanadate, β-glycerophosphate, aprotinin, leupeptin, Protein A-Sepharose CL-4B, and anti-FLAG and anti-MYC antibodies were purchased from Sigma. H2B and MBP were purchased from Roche Biochemicals. [^{32}P]α-ATP and [^{32}P]γ-ATP were purchased from ICN. Secondary antibodies and Glutathione Sepharose were obtained from Amersham Pharmacia.

Creation of the shk1 *null strain*

An *shk1* knockout construct was made by inserting the Blasticidin (*Bsr*) resistance (Sutoh 1993) cassette into the *Bam*HI site (nucleotide position 848 of the *shk1* ORF) of a full-length *shk1* construct in pAT153. The knockout construct was digested with *Sal*1 and *Eco*RV and transformed into *Dictyostelium* cells. After Bsr selection, cells were plated on bacteria (*Klebsiella aerogenes*) for isolation of clones. Two clones were observed to form abnormally small plaques and fruiting bodies. These

clones, along with randomly picked ones, were examined by Southern blot analysis of their genomic DNA digested with *Bcl*1 and probed with a 3′-end fragment of *shk1* that encodes the SH2 domain. Both clones that formed the small plaques were found to have a *Bsr* insertion in the endogenous *shk1*. Subsequent Northern blot analysis verified the absence of an *shk1* message. Transformation of an SHK1 expression construct into the *shk1* null cells complemented the *shk1* null developmental phenotypes.

Plasmids

Part of the *shk1* nucleotide sequence was obtained from the *Dictyostelium* cDNA sequencing project at the University of Tsukuba, Japan. This sequence information was used to amplify a probe from genomic DNA by PCR. A full-length *shk1* cDNA clone was obtained by screening a 12- to 16-h developmental λZAP library (Schnitzler et al. 1994) and cloned into the *Eco*RI site of pBluescript.

For the FLAG–SHK1 construct, the primers GTTTTTAG ATCTAAAAATGGATTATAAAGATGACGATGACAAACA AATTAAGGCTAGAAAAG and GTTTTTCTCGAGTTAAT TGATGTAACCAGATAATTG were used in a PCR reaction with the *shk1* cDNA as a template. The resulting PCR product was digested with *Bgl*II and *Xho*I and cloned into the *Dictyostelium* expression vector EXP-4+ and sequenced to verify the ORF.

For the myristoylation, FLAG–SHK1 construct primers GTTTTTGTCAACAGATTATAAAGATGACGATGAC and GT TTTTCTCGAGTTAATTGATGTAACCAGATAATTG were used in a PCR reaction with the FLAG–SHK1 construct as the template. The PCR product was digested with *Hinc*II and *Xho*I and cloned into pRM8-4, resulting in myristoylation signal (a membrane targeting epitope of c-Src) incorporation (Meili et al. 1999).

The SHK1^{R449A} (SH2 domain mutant R449A) was generated using the Transformer site-directed mutagenesis kit (Clonetech) with the oligonucleotide GTTGAGAAAGCCACTAA AAATGTAC employed to introduce the desired mutation. We confirmed successful mutagenesis by sequencing.

For the GST–SHK1 construct, the primers GTTTTTC TAGACCAAATTAAGGCTAGAAAAG and GTTTTTCTCG AGTTAATTGATGTAACCAGATAATTG were used in a PCR reaction with *shk1* as the template. The PCR product was digested with *Xba*I and *Xho*I and cloned into pGEX-KG for expression in *E. coli*.

The CRAC–GFP construct was a generous gift from Carole Parent and Peter Devreotes (Johns Hopkins University; Parent et al. 1998). Coronin–GFP was a generous gift from G. Gerisch (Gerisch et al. 1995). PhdA–GFP and PKB–GFP were constructed as described by S. Funamoto and R.A. Firtel (unpubl.) and Meili et al. (1999), respectively.

Aggregation-competent cells

To produce cells competent to respond to cAMP (aggregation-competent cells), log-phase, axenically grown cells were washed in Na/K phosphate buffer and resuspended at a density of 5×10^6 cells/mL in Na/K phosphate buffer and pulsed for 5 h with 30 nM cAMP every 10 min (Devreotes et al. 1987; Ma et al. 1997).

Cellular responses to cAMP stimulation

To observe the behavior of aggregation-competent cells in a cAMP gradient, cells were plated in Na/K phosphate buffer at a density of 6×10^4 cells/cm^2 onto a plate with a hole covered by a 0.17-mm glass coverslip. An Eppendorf Patchman micromanipulator with a glass capillary needle filled with 150 μM cAMP was brought into the field of view of a Nikon Eclipse TE inverted microscope and placed near the cells to establish a gradient as previously described (Chung and Firtel 1999; Meili et al. 1999). Visible and fluorescent images of chemotaxing cells were digitally recorded and processed as previously described (Chung and Firtel 1999; Meili et al. 1999), except for the fluorescent images that were acquired and processed using the Metamorph imaging system (Scanalytics, Universal Imaging Corp.).

To observe the effect of global cAMP stimulation on chemotaxis-competent cells, the cells were treated as described above except that instead of using a glass capillary to establish a cAMP gradient, the cells were stimulated with a pulse of 150 nM cAMP. Fluorescent images were acquired and processed using the Metamorph imaging system.

Quantitation of membrane or cortical localization of GFP fusion of PH-domain-containing proteins and coronin–GFP in wild-type cells, *pi3k1/2* null cells, *phdA* null cells, and wild-type cells treated with LY294002 represents the averages of at least five cells from at least three separate experiments. A CCD camera (SenSys Photometrics) was used to capture fluorescent images. The pictures were acquired and analyzed using Metamorph software. The intensity of cortical GFP was measured by line scanning with the Metamorph software. The level of cortical GFP was calculated by dividing intensity before stimulation (E_0) by intensity at each time point (E) after subtraction of the basal intensity.

To asssay PKB activity, cells were lysed and PKB was immunoprecipitated and assayed for activity as previously described by Meili et al. (1999).

SHK1 kinase activity in response to cAMP stimulation was assayed using a protocol similar to methods previously described for PKB and PAKa (Chung et el. 1998; Meili et al. 1999). Briefly, aggregation-competent cells expressing FLAG-tagged SHK1 were stimulated with cAMP and aliquots were taken at specified times. Cells were immediately lysed in the presence of protease and phosphatase inhibitors and FLAG–SHK1 was immunoprecipitated using an anti-FLAG antibody and assayed for kinase activity using Histone 2B (H2B) as a substrate. Reaction mixtures were sized by SDS-PAGE, and the level of $^{32}PO_4$ incorporation into the H2B band was examined by autoradiography and quantified by densitometry tracing and/or using a phosphoimager. Time points were taken at 0 (before stimulation), 5, 10, 20, 30, 40, 60, 120, and 480 sec. See Meili et al. (1999) and Chung et al. (1998) for details.

Phagocytosis

Phagocytosis was measured as previously described (Seastone et al. 1999). To determine the amount and rate of bacterial uptake, *Dictyostelium* cell lines grown axenically in log phase were adjusted to a concentration of 1×10^6 cells/mL in a suspension of GFP-tagged *E. coli* (a gift from Roger Tsien, UCSD) and allowed to feed on the bacteria. *Dictyostelium* cell samples were isolated by differential centrifugation, fixed in 3.7% formaldehyde, and bacterial uptake was quantified on a Fluoromax fluorometer.

To quantify the ability of *Dictyostelium* cell lines to grow on bacteria, cells were adjusted to a concentration of 1×10^6 cells/mL in an *E. coli* suspension. Bacterial clearing was quantified by measuring turbidity at OD_{595}.

To ascertain the rate of phagocytosis of *Dictyostelium* cell lines, 1×10^5 axenically grown cells were placed on a glass slide in a suspension of Na/K phosphate buffer, and 2-μm FluoSphere

beads were added to the suspension (to a final concentration of 2×10^3% solids). Bead internalization by the cells was digitally recorded by visible and fluorescence microscopy as described above. The time it took for cells to internalize beads was measured from the moment a bead attached to the exterior of the cell to the moment it was completely internalized as determined by the analysis of the digital videomicroscopic recordings. Cells that were thought to have taken up beads were recorded for several minutes further as they moved along the slide to ensure the beads were actually in the cells.

In vivo actin polymerization assay

In vivo F-actin levels were quantified according to Zigmond et al. (1997). Briefly, aggregation-competent cells were resuspended at 1×10^7 cells/mL in Na/K phosphate buffer and shaken at 200 rpm with 2.5 mM caffeine (to block endogenous cAMP oscillations) for 20 min. Cells were then spun and resuspended in Na/K phosphate buffer and stimulated with 100 nM cAMP. Cell samples (500 µL) were taken at 0, 5, 10, 15, 20, 30, and 60 sec after cAMP stimulation and mixed with actin buffer (20 mM KH_2PO_4, 10 mM Pipes at pH 6.8, 5 mM EGTA, 2 mM $MgCl_2$) containing 6% formaldehyde, 0.15% Triton X-100, and 1 mM tetramethylrhodamine B isothiocyanate phalloidin. Cells were fixed and stained for 1 h at room temperature, then spun down in the microcentrifuge, and the supernatant was aspirated off and the sample washed with actin buffer. Next 1 mL of 100% methanol was added to the pelleted cells, and fluorescence was quantified on a Fluoromax fluorometer (540 excitation, 575 emission). To determine nonsaturatable binding, 100 mM unlabeled phalloidin was included.

Phalloidin and immunofluorescence staining

Dictyostelium cells were fixed in 3.7% formaldehyde, permeabilized in 0.1% Triton X, and stained with either anti-FLAG antibody or TRITC-phalloidin. FITC-anti-mouse secondary antibody was used to visualize the anti-FLAG staining. Fluorescent pictures were obtained with a Microphot FX microscope by digital acquisition using IPLab Spectrum software (Scanalytics, Universal Imaging Corp.).

Phosphoamino acid analysis

The *E. coli*-expressed GST fusion protein of SHK1 was purified using glutathione beads. We used the fusion protein to phosphorylate MBP and H2B. The kinase reactions were subjected to SDS-PAGE, transferred to PVDF membrane, and subjected to phosphoamino acid analysis as described by Biggs et al. (1999).

Acknowledgments

We thank members of the Firtel lab for helpful discussions and Jennifer Roth for critical reading of the manuscript. J.M. was supported in part by a postdoctoral fellowship from the Canadian Institutes of Health Research (CIHR). This work was supported by grants to J. Williams, T. Hunter, and R.A. Firtel.

The publication costs of this article were defrayed in part by payment of page charges. This article must therefore be hereby marked "advertisement" in accordance with 18 USC section 1734 solely to indicate this fact.

References

Adler, K., Gerisch, G., von Hugo, U., Lupas, A., and Schweiger, A. 1996. Classification of tyrosine kinases from *Dictyostelium discoideum* with two distinct, complete or incomplete catalytic domains. *FEBS Lett.* **395:** 286–292.

Alessi, D., Andjelkovic, M., Caudwell, B., Cron, P., Morrice, N., Cohen, P., and Hemmings, B. 1996. Mechanism of activation of protein kinase B by insulin and IGF-1. *EMBO J.* **15:** 6541–6551.

Alessi, D., James, S., Downes, C., Holmes, A., Gaffney, P., Reese, C., and Cohen, P. 1997. Characterization of a 3-phosphoinositide-dependent protein kinase which phosphorylates and activates protein kinase Bα. *Curr. Biol.* **7:** 261–269.

Andjelkovic, M., Alessi, D.R., Meier, R., Fernandez, A., Lamb, N.J., Frech, M., Cron, P., Cohen, P., Lucocq, J.M., and Hemmings, B.A. 1997. Role of translocation in the activation and function of protein kinase B. *J. Biol. Chem.* **272:** 31515–31524.

Biggs, W.H., III, Meisenhelder, J., Hunter, T., Cavenee, W.K., and Arden, K.C. 1999. Protein kinase B/Akt-mediated phosphorylation promotes nuclear exclusion of the winged helix transcription factor FKHR1. *Proc. Natl. Acad. Sci. USA* **96:** 7421–7426.

Buczynski, G., Grove, B., Nomura, A., Kleve, M., Bush, J., Firtel, R.A., and Cardelli, J. 1997. Inactivation of two *Dictyostelium discoideum* genes, *DdPIK1* and *DdPIK2*, encoding proteins related to mammalian phosphatidylinositide 3-kinases, results in defects in endocytosis, lysosome to postlysosome transport, and actin cytoskeleton organization. *J. Cell Biol.* **136:** 1271–1286.

Buser, C., Sigal, C., Resh, M., and McLaughlin, S. 1994. Membrane binding of myristylated peptides corresponding to the NH2 terminus of Src. *Biochemistry* **33:** 13093–13101.

Chung, C.Y. and Firtel, R.A. 1999. PAKa, a putative PAK family member, is required for cytokinesis and the regulation of the cytoskeleton in *Dictyostelium discoideum* cells during chemotaxis. *J. Cell Biol.* **147:** 559–575.

Coffer, P.J., Jin, J., and Woodgett, J.R. 1998. Protein kinase B (c-Akt): A multifunctional mediator of phosphatidylinositol 3-kinase activation. *Biochem. J.* **335:** 1–13.

de Hostos, E.L., Bradtke, B., Lottspeich, F., Guggenheim, R., and Gerisch, G. 1991. Coronin, an actin binding protein of *Dictyostelium discoideum* localized to cell surface projections, has sequence similarities to G-protein β-subunits. *EMBO J.* **10:** 4097–4104.

Devreotes, P., Fontana, D., Klein, P., Sherring, J., and Theibert, A. 1987. Transmembrane signaling in *Dictyostelium*. *Meth. Cell Biol.* **28:** 299–331.

Firtel, R.A. and Chung, C.Y. 2000. The molecular genetics of chemotaxis: Sensing and responding to chemoattractant gradients. *BioEssays* **22:** 603–615.

Frech, M., Andjelkovich, M., Ingley, E., Reddy, K., Falck, J., and Hemmings, B. 1997. High affinity binding of inositol phosphatase and phosphoinositides to the pleckstrin homology domain of RAC/protein kinase B and their influence on kinase activity. *J. Biol. Chem.* **272:** 8474–8481.

Fruman, D.A., Rameh, L.E., and Cantley, L.C. 1999. Phosphoinositide binding domains: Embracing 3-phosphate. *Cell* **97:** 817–820.

Fu, X.-Y. and Zhang, J.-J. 1993. Transcription factor p91 interacts with the epidermal growth factor receptor and mediates activation of the c-*fos* gene promoter. *Cell* **74:** 1135–1145.

Fukui, Y., De Lozanne, A., and Spudich, J.A. 1990. Structure and function of the cytoskeleton of a *Dictyostelium* myosin-defective mutant. *J. Cell Biol.* **110:** 367–378.

Gerisch, G., Albrecht, R., Heizer, C., Hodgkinson, S., and Maniak, M. 1995. Chemoattractant-controlled accumulation of coronin at the leading edge of *Dictyostelium* cells monitored using green fluorescent protein–coronin fusion protein.

Curr. Biol. **5:** 1280–1285.
Hirsch, E., Katanaev, V.L., Garlanda, C., Azzolino, O., Pirola, L., Silengo, L., Sozzani, S., Mantovani, A., Altruda, F., and Wymann, M.P. 2000. Central role for G protein-coupled phosphoinositide 3-kinase γ in inflammation. *Science* **287:** 1049–1053.
Jungbluth, A., Eckerskorn, C., Gerisch, G., Lottspeich, F., Stocker, S., and Schweiger, A. 1995. Stress-induced tyrosine phosphorylation of actin in *Dictyostelium* cells and localization of the phosphorylation site to tyrosine-53 adjacent to the DNase I binding loop. *FEBS Lett.* **375:** 87–90.
Kawata, T., Shevchenko, A., Fukuzawa, M., Jermyn, K.A., Totty, N.F., Zhokovskaya, N.V., Sterling, A.E., Mann, M., and Williams, J.G. 1997. SH2 signaling in a lower eukaryote: A STAT protein that regulates stalk cell differentiation in *Dictyostelium*. *Cell* **89:** 909–916.
Kim, L., Liu, J.C., and Kimmel, A.R. 1999. The novel tyrosine kinase ZAK1 activates GSK3 to direct cell fate specification. *Cell* **99:** 399–408.
Klippel, A., Kavanaugh, W.M., Pot, D., and Williams, L.T. 1997. A specific product of phosphatidylinositol 3-kinase directly activates the protein kinase Akt through its pleckstrin homology domain. *Mol. Cell. Biol.* **17:** 338–344.
Kohn, A.D., Summers, S.A., Birnbaum, M.J., and Roth, R.A. 1996. Expression of a constitutively active Akt Ser/Thr kinase in 3T3-L1 adipocytes stimulates glucose uptake and glucose transporter 4 translocation. *J. Biol. Chem.* **271:** 31372–31378.
Leevers, S.J., Vanhaesebroeck, B., and Waterfield, M.D. 1999. Signaling through phosphoinositide 3-kinases: The lipids take centre stage. *Curr. Opin. Cell Biol.* **11:** 219–225.
Li, Z., Jiang, V., Xie, W., Zhang, Z., Smrcka, A.V., and Wu, D. 2000. Roles of PLC-β2 and -β3 and PI3Kγ in chemoattractant-mediated signal transduction. *Science* **287:** 1046–1049.
Ma, H., Gamper, M., Parent, C., and Firtel, R.A. 1997. The *Dictyostelium* MAP kinase kinase DdMEK1 regulates chemotaxis and is essential for chemoattractant-mediated activation of guanylyl cyclase. *EMBO J.* **16:** 4317–4332.
Meili, R., Ellsworth, C., Lee, S., Reddy, T.B., Ma, H., and Firtel, R.A. 1999. Chemoattractant-mediated transient activation and membrane localization of Akt/PKB is required for efficient chemotaxis to cAMP in *Dictyostelium*. *EMBO J.* **18:** 2092–2105.
Meili, R., Ellsworth, C., and Firtel, R.A. 2000. A novel Akt/PKB-related kinase is essential for morphogenesis in *Dictyostelium*. *Curr. Biol.* **10:** 708–717.
Nuckolls, G.H., Osherov, N., Loomis, W.F., and Spudich, J.A. 1996. The *Dictyostelium* dual-specificity kinase splA is essential for spore differentiation. *Development* **122:** 3295–3305.
Parent, C.A. and Devreotes, P.N. 1999. A cell's sense of direction. *Science* **284:** 765–770.
Parent, C.A., Blacklock, B.J., Froehlich, W.M., Murphy, D.B., and Devreotes, P.N. 1998. G protein signaling events are activated at the leading edge of chemotactic cells. *Cell* **95:** 81–91.
Rameh, L.E. and Cantley, L.C. 1999. The role of phosphoinositide 3-kinase lipid products in cell function. *J. Biol. Chem.* **274:** 8347–8350.
Rameh, L.E., Chen, C.S., and Cantley, L.C. 1995. Phosphatidylinositol (3,4,5)P_3 interacts with SH2 domains and modulates PI 3-kinase association with tyrosine-phosphorylated proteins. *Cell* **83:** 821–830.
Rickert, P., Weiner, O.D., Wang, F., Bourne, H.R., and Servant, G. 2000. Leukocytes navigate by compass: Roles of PI3K and its lipid products. *Trends Cell Biol.* **10:** 466–473.
Salinas, M., López-Valdaliso, R., Martín, D., Alvarez, A., and Cuadrado, A. 2000. Inhibition of PKB/Akt1 by C2-ceramide involves activation of ceramide-activated protein phosphatase in PC12 cells. *Mol. Cell. Neurosci.* **15:** 156–169.
Sanchez-Madrid, F. and del Pozo, M.A. 1999. Leukocyte polarization in cell migration and immuneinteractions. *EMBO J.* **18:** 501–511.
Sasaki, T., Irie-Sasaki, J., Jones, R.G., Oliveira-dos-Santos, A.J., Stanford, W.L., Bolon, B., Wakeham, A., Itie, A., Bouchard, D., Kozieradzki, I., et al. 2000. Function of PI3Kγ in thymocyte development, T cell activation, and neutrophil migration. *Science* **287:** 1040–1046.
Seastone, D.J., Zhang, L.Y., Buczynski, G., Rebstein, P., Weeks, G., Spiegelman, G., and Cardelli, J. 1999. The small Mr Ras-like GTPase Rap1 and the phospholipase C pathway act to regulate phagocytosis in *Dictyostelium discoideum*. *Mol. Biol. Cell* **10:** 393–406.
Servant, G., Weiner, O.D., Herzmark, P., Balla, T., Sedat, J.W., and. Bourne, H.R 2000. Polarization of chemoattractant receptor signaling during neutrophil chemotaxis. *Science* **287:** 1037–1040.
Shual, K., Ziemiecki, A., Wilks, A.F., Harpur, A.G., Sadowski, H.B., Gilman, M.Z., and Darnell, J.E. 1993. Polypeptide signaling to the nucleus through tyrosine phosphorylation of Jak and Stat proteins. *Nature* **366:** 580–583.
Sigal, C., Zhou, W., Buser, C., McLaughlin, S., and Resh, M. 1994. Amino-terminal basic residues of Src mediate membrane binding through electrostatic interaction with acidic phospholipids. *Proc. Natl. Acad. Sci. USA* **91:** 12253–12257.
Soll, D. and Voss, E. 1998. Two- and three-dimensional computer systems for analyzing how animal cells crawl. In *Motion analysis of living cells* (eds. D. Soll and D. Wessels), pp. 25–52. Wiley-Liss, New York.
Stockoe, D., Stephens, L., Copeland, T., Gaffney, P., Reese, C., Painter, G., Holmes, A., McCormick, F., and. Hawkins, P. 1997. Dual role of phosphatidylinositol-3,4,5-triphosphate in the activation of protein kinase B. *Science* **277:** 567–570.
Sutoh, K. 1993. A transformation vector for *Dictyostelium discoideum* with a new selectable marker Bsr. *Plasmid* **30:** 150–154.
Tilton, B., Andjelkovic, M., Didichenko, S.A., Hemmings, B.A., and Thelen, M. 1997. G-Protein-coupled receptors and Fcγ-receptors mediate activation of Akt/protein kinase B in human phagocytes. *J. Biol. Chem.* **272:** 28096–-28101.
Vanhaesebroeck, B. and Waterfield, M.D. 1999. Signaling by distinct classes of phosphoinositide 3-kinases. *Exp. Cell Res.* **253:** 239–254.
Vanhaesebroeck, B., Jones, G.E., Allen, W.E., Zicha, D., Hooshmand-Rad, R., Sawyer, C., Wells, C., Waterfield, M.D., and Ridley, A.J. 1999. Distinct PI(3)Ks mediate mitogenic signalling and cell migration in macrophages. *Nature Cell Biol.* **1:** 69–71.
Wessels, D. and Soll, D.R. 1998. Computer-assisted characterization of the behavioral defects of cytoskeletal mutants of *Dictyostelium discoideum*. In *Motion analysis of living cells* (eds. D. Soll and D. Wessels), pp. 101–140. Wiley-Liss, New York.
Zigmond, S.H., Joyce, M., Borleis, J., Bokoch, G.M., and Devreotes, P.N. 1997. Regulation of actin polymerization in cell-free systems by GTPγS and Cdc42. *J. Cell Biol.* **138:** 363–374..